Enzyme Inhibition

DOI: 10.1002/ange.201102965

Development of Highly Potent Inhibitors of the Ras-Targeting Human Acyl Protein Thioesterases Based on Substrate Similarity Design

*Christian Hedberg, Frank J. Dekker, Marion Rusch, Steffen Renner, Stefan Wetzel, Nachiket Vartak, Claas Gerding-Reimers, Robin S. Bon, Philippe I. H. Bastiaens, and Herbert Waldmann**

Signal-transducing Ras guanine nucleotide binding proteins (GTPases) play important roles in decisive cellular processes, such as growth, division, and differentiation.[1,2] Mutations in the *S*-farnesylated and *S*-palmitoylated H- and N-Ras isoforms result in oncogenic activation, which frequently occurs in melanoma, leukemia, and cancers of the bladder, liver, and kidney.[3]

S-Palmitoylation is required to maintain proper Ras localization in cells,[4,5] and a dynamic de-/repalmitoylation cycle determines the trafficking and the spatiotemporal signaling profile of H- and N-Ras, thus regulating the amplitude, duration, and coupling to different signaling pathways and effectors.[6] The dynamic nature of the cycle is established by palmitoyl transferases and thioesterases, and recently, acyl protein thioesterase 1 (APT1) has been proven to be a major H- and N-Ras depalmitoylating enzyme in cells.[7,8]

Chemical interference with the dynamic Ras de/reacylation cycle by using the β-lactone APT1 inhibitor palmostatin B (Figure 1) disturbs the precise steady-state localization of H- and N-Ras, thereby causing unspecific entropy-driven redistribution to endomembranes, and down-regulation of global Ras signaling.[7] However, it remains unclear if APT1 is the only Ras-depalmitoylating enzyme in cells and whether palmostatin B targets additional proteins relevant to the Ras acylation cycle, in particular the closely related isoenzyme APT2.[9]

Herein we describe the substrate-based design of novel β-lactone inhibitors of Ras depalmitoylation which led to the development of the highly potent APT inhibitor palmostatin M (**30**, Table 1). In the following manuscript,[10] we detail the development of activity-based probes based on palmostatin M and B as well as their use in chemical proteomics experiments, which have revealed both APT1 and APT2 as the targets relevant to the dynamic Ras acylation cycle.

The APT1 inhibitor palmostatin B was identified by employing the chemical structure based principles of protein structure similarity clustering (PSSC)[11,12] and biology-oriented synthesis,[13–15] namely the structural similarity among ligand-sensing cores of proteins and of related classes of potential inhibitors. However, APT1 is a cytosolic enzyme[16–19] with very broad substrate scope. It not only depalmitoylates the C terminus of small GTPases, in both D- and L-amino acid forms,[8] but also other G proteins,[20,21] ghrelin (deoctanoylation),[22] viral glycoproteins,[23] and lysophospholipids.[18] This very unusual and exceptionally wide substrate tolerance inspired us to alternatively employ the structural characteristics of the different substrates as guiding arguments for the design of a more potent family of inhibitors. The activity of palmostatin B is mainly determined by the stereochemistry of its electrophilic β-lactone core and the aliphatic substitution at its α position. Ideation based on substrate similarity indicates that selective recognition will be enhanced by the introduction of functionalities that enable hydrogen bonding and electrostatic interactions to the β position (Figure 1).

We compared two known native APT1 substrates, lysophospholipid **1** and the H-Ras C terminus **2**, and identified a common recognition motif that consists of a negatively charged group at a distance of five to six bonds (red) from the (thio-)ester functionality (green) and a positively charged tail group ten to twelve bonds away (blue) (Figure 1a). We found that the phosphatidyl choline moiety **3** (Figure 1b) fulfilled the design requirements to provide the required electrostatic interactions. However, since the zwitterionic nature of the phosphatidyl choline moiety might limit application in cells, it was replaced by a sulfonyl-1,3-propylene-*N,N*-dimethylamino functionality **4** (Figure 1b). We fused fragment **4** through a variable spacer to a *trans*-β-

[*] Dr. C. Hedberg, Dipl.-Chem. M. Rusch, Dr. C. Gerding-Reimers, Prof. Dr. H. Waldmann
Max-Planck-Institut für molekulare Physiologie
Abt. Chemische Biologie
Otto-Hahn-Strasse 11, 44227 Dortmund (Germany)
and
Technische Universität Dortmund, Fakultät Chemie
Lehrbereich Chem. Biologie
Otto-Hahn-Strasse 6, 44227 Dortmund (Germany)
E-mail: herbert.waldmann@mpi-dortmund.mpg.de
Dr. F. J. Dekker
Univ. of Groningen, University Centre for Pharmacy
A. Deusinglaan 1, 9713 AV Groningen (The Netherlands)
Dr. S. Renner, Dr. S. Wetzel
Novartis Pharma AG, Novartis Institute of Biomedical Research
4056 Basel (Switzerland)
Dr. R. S. Bon
School of Chemistry, University of Leeds and
Biomedical and Health Research Centre
LS2 9JT Leeds (UK)
Dr. N. Vartak, Prof. Dr. P. I. H. Bastiaens
Max-Planck-Institut für molekulare Physiologie
Abt. Systemische Zellbiologie
Otto-Hahn-Strasse 11, 44227 Dortmund (Germany)

Supporting information for this article is available on the WWW under http://dx.doi.org/10.1002/anie.201102965.

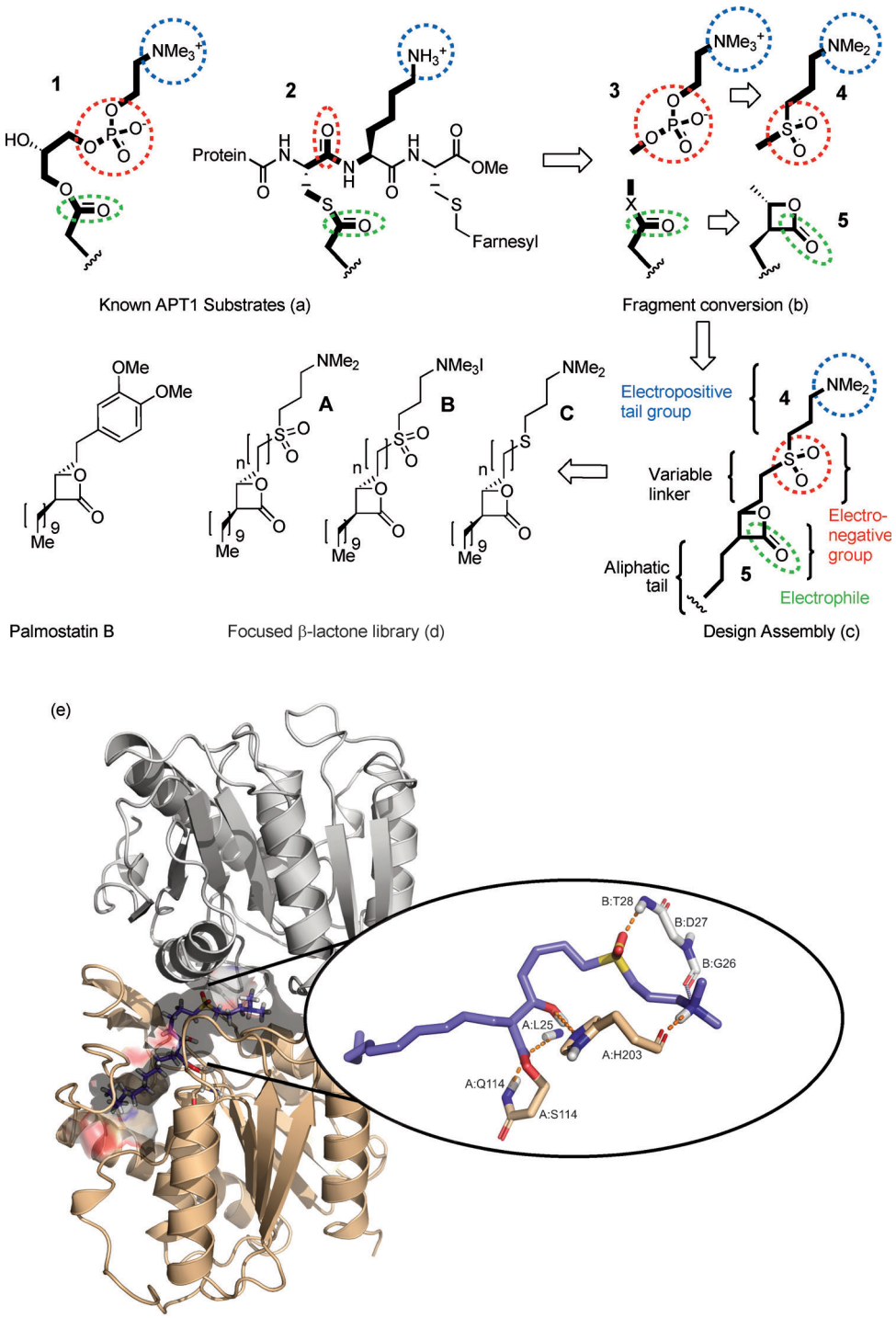

Figure 1. Inhibitor development based on substrate similarity.

lactone core **5**, which addresses the stereochemical preference of APT1[7] and serves as a covalent modifier of the nucleophilic residue in the active site of the enzyme. Variation of the spacer length enables identification of the optimal distance between fragments **4** and **5**. A lipophilic tail mimicking the palmitate moiety was introduced on the opposite side of the β-lactone core to create affinity to the lipid-binding pocket of the enzyme[24] (Figure 1c). Based on these criteria, we designed a small focused library of three series of inhibitors, denoted A–C, which would define the structure–activity relationship (Figure 1d). The design was further verified in silico by modeling the binding mode through electrostatic interactions in the active site of the APT1 *apo*-crystal structure.[25] In silico, the polar residues Q114 and L25 make strong interactions to the opened β-lactone, in which the carbonyl group is covalently bound to the nucleophilic S114. Notably, the polar head group of the inhibitor makes contact with residues T28 and H203, thus creating an electrostatic stabilizing interaction (Figure 1e).

The synthesis of the inhibitor commenced with the dicyclohexylboron triflate mediated *anti*-aldol reaction[26] between the *O*-dodecylated ephedrine auxiliaries **6** and **7** with aldehydes **8**–**11** (Scheme 1, and see the Supporting Information). The whole synthesis sequence was carried out with both enantiomers of the ephedrine auxiliary, thus resulting in two series, denoted (*S*,*S*) and (*R*,*R*), of reaction products as single enantiomers. The aldol reaction products were purified to diastereomeric homogeneity by column chromatography to yield compounds **12**–**19**. A subsequent *S* oxidation of **12**–**19** with peracetic acid yielded the corresponding sulfones, which were not isolated. Some overoxidation on the amine functionality occurred (*N*-oxide formation); however, brief treatment with H_2 over Pd/C in MeOH reduced the *N*-oxides quantitatively back to the amines. Removal of the auxiliary from the crude sulfones by hydrogenolysis over Pearlmans catalyst ($Pd(OH)_2$/C) at slightly elevated temperature (40 °C) provided the free β-hydroxy acids **20**–**27** without epimerization. A subsequent β-lactonization with phenylsulfonyl chloride/pyridine concluded the synthesis of sublibrary A (**28**–**35**). Series A (**28**–

Table 1: IC_{50} values for the inhibition of APT1 by the focused β-lactone libraries A–C.[a]

Compound (*S*,*S*)	IC_{50} APT1 [nM]	Compound (*R*,*R*)	IC_{50} APT1 [nM]
A			
28: $n=2$	6.75 ± 0.53	**32**: $n=2$	42.20 ± 2.27
29: $n=3$	3.98 ± 0.13	**33**: $n=3$	37.27 ± 1.91
30: $n=4$	2.13 ± 0.31	**34**: $n=4$	20.46 ± 3.04
31: $n=5$	2.96 ± 0.48	**35**: $n=5$	28.18 ± 4.48
B			
36: $n=3$	2.65 ± 0.15	**39**: $n=3$	38.32 ± 2.33
37: $n=4$	1.67 ± 0.28	**40**: $n=4$	23.61 ± 0.58
38: $n=5$	1.30 ± 0.07	**41**: $n=5$	17.38 ± 1.65
C			
50: $n=2$	5.93 ± 0.79	**53**: $n=2$	22.06 ± 3.02
51: $n=4$	5.61 ± 0.74	**54**: $n=4$	34.15 ± 4.84
52: $n=5$	6.36 ± 0.88	**55**: $n=5$	29.83 ± 3.18

[a] All IC_{50} values were determined with DiFMUO as substrate, and released DiFMU was observed by the increase in the fluorescence intensity at 510 nm. Data were determined by at least three independent measurements. *Z*′ factors were in all cases higher than 0.65. Inhibition curves are given in the Supporting Information.

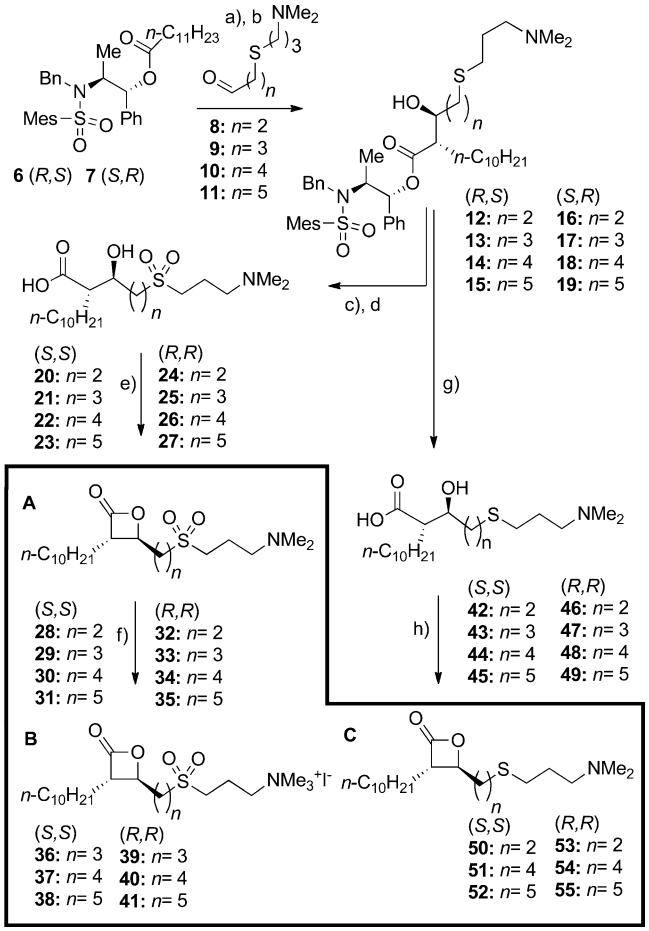

Scheme 1. Synthesis of a β-lactone library. Reagents and conditions: a) $(CyHex)_2BOTf$ (2.2 equiv), Et_3N (1.5 equiv), CH_2Cl_2, −78 °C (2 h); b) aminoaldehyde (1.1 equiv), CH_2Cl_2, −78 °C (1 h) then 0 °C (1 h), 60–80% over 2 steps; c) 3 equiv AcO_2H, MeOH, RT (3 h); d) 20 mol% $Pd(OH)_2/C$, H_2, MeOH, 40 °C, 24 h, 55–85% over 2 steps; e) $PhSO_2Cl$ (2 equiv), pyridine, 0 °C, overnight, 50–80%; f) MeI (4 equiv), MeCN, RT, 3 h, quantitative; g) LiOH (3 equiv), dioxane/MeOH/H_2O (8:1:1), RT, 48 h, 65–73%; h) $PhSO_2Cl$ (2 equiv), pyridine, 0 °C, overnight, 60–82%. CyHex = cyclohexyl, OTf = trifluoromethanesulfonyl.

35) was quarternized at the dimethylamino functionality by treatment with an excess of methyl iodide in acetonitrile to yield sublibrary B (**36**–**41**). To validate the design principle, a third sublibrary (C), not carrying the polar sulfone moiety, was prepared. The auxiliary was removed from intermediates **12**–**19** under basic conditions, thereby yielding β-hydroxy acids **42**–**49**, which were subjected to subsequent β-lactonization (**50**–**55**).

To identify and characterize APT1 inhibitors, focused β-lactone libraries (A–C) were screened for inhibitory activity of recombinant hAPT1 by employing 7-octoyl-6,8-difluoroumbelliferone (DiFMUO) as the substrate. The released 6,8-difluoroumbelliferone (DiFMU) was detected by the increase in fluorescence intensity at 510 nm. IC_{50} values were determined to estimate the residual enzyme activity after preincubation with inhibitors. We identified the (*S*,*S*)-β-lactones in sublibraries A (**28**–**31**, Table 1) and B (**36**–**38**, Table 1) as highly potent inhibitors, and the postulated importance of the spacer length between the β-lactone core and the polar head group was verified. Investigation of the APT1 inhibitory activity also revealed a crucial role of the sulfone moiety; thus replacement by a sulfide (series C) led to a decrease in activity. The *S*,*S* compounds with a spacer length of 4 or 5 carbon atoms from series A and B proved to be most potent, with IC_{50} values of about 2.5 nM. In comparison, palmostatin B displays an IC_{50} value of 5.4 nM under identical assay conditions. Investigation of the enzyme kinetics upon treatment of APT1 with the most potent compound (**30**) from sublibrary A revealed an apparent competitive mode of inhibition. This finding indicates a similar binding mechanism as observed for palmostatin B, in which the enzyme is quickly inactivated by covalent acylation by the inhibitor, followed by a relatively slow reactivation by hydrolysis of the acyl–enzyme intermediate. We verified the importance of the β-lactone core (see the following manuscript for details). Briefly, IC_{50} values were shifted by a factor of about 1000 upon hydrolysis of the β-lactone, or by converting it into the corresponding methyl ester.[10] In addition, the initial pre-steady-state kinetics for inactivation of the enzyme was fast (rate constant greater than $5\times10^3\ mol^{-1}\,s^{-1}$), and the half-life ($t_{1/2}$) of the enzyme–inhibitor complex was in the range of 2–3 min (see the Supporting Information), similar to that of palmostatin B.

To verify the results of the biochemical assay in cells, the three β-lactone sublibraries were subjected to a MDCK-F3 back-transformation assay,[27,28] in which HRasG12V-transformed MDCK-F3 cells were subjected to chronic overnight

incubation with a high, but noncytotoxic concentration of each inhibitor (30 μM, see the Supporting Information). Down-regulation of oncogenic Ras signaling in these cells would result in a partial phenotypic reversion,[7] including a change from a spindle-shaped to a more round-shaped cell morphology and restoration of cell adhesion and cadherin expression at the cell–cell contact sites. Under these conditions, only compounds from sublibrary A (more potent) and C (less potent) induced the expected reversion from the spindlelike to the round-shaped phenotype of untransformed MDCK cells. This behavior is comparable to treatment with the specific MEK inhibitor U0126,[29] a known blocker of the MAP-kinase pathway downstream of Ras. This result indicates that cationic sublibrary B, which provided potent APT1 inhibitors in the biochemical assay, has no or minor activity in cells, possibly because of poor cell permeability. Immunostaining for E-cadherin expression at the cell surface[27] to quantify the degree of phenotypic reversion by the expression level of E-cadherin revealed that **30** is distinctly more potent than palmostatin B (Figure 2A). In light of these findings, we chose **30** as the most potent inhibitor for further characterization and termed it palmostatin M.

Inhibition of APT1 leads to an interruption of dynamic Ras trafficking between the Golgi and the plasma membrane, since palmitoylated Ras cannot be retrapped kinetically at the Golgi and subsequently directed to the plasma membrane through the secretory pathway.[7] To show that palmostatin M interrupts the dynamic Ras de/reacylation cycle, we treated MDCK cells expressing the fluorescent protein fusion constructs mCitrine-*N*-Ras, mCitrine-H-Ras, or mCitrine-K-Ras,

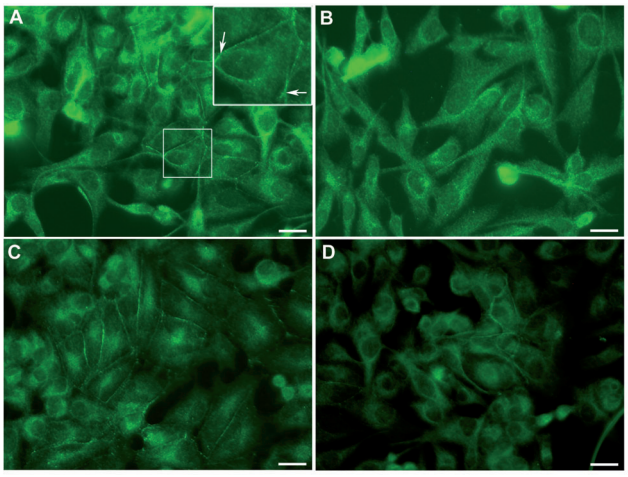

Figure 2. Characterization of palmostatin M (**30**) in cells. A) E-cadherin immunostaining of HRasG12V-transformed MDCK-F3 cells showing restoration of E-cadherin expression at the cell–cell interfaces (arrowheads) after treatment with 10 μM palmostatin M. B) DMSO control. C) HRasG12V-transformed MDCK-F3 cells treated with palmostatin B at 50 μM show a similar, but weaker effect on the phenotype. D) Treatment of HRasG12V-transformed MDCK-F3 cells with the known MEK inhibitor U0126 as a positive control. MDCK cells (non-HRasG12V transformed) treated with DMSO and palmostatin B (50 μM) are controls for the reversed phenotype (see the Supporting Information). Scale bars represent 20 μm.

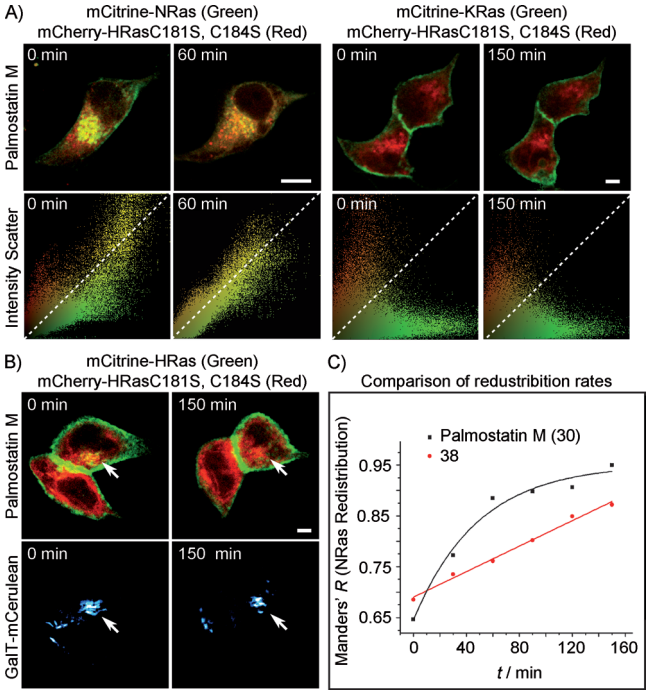

Figure 3. Palmostatin M (**30**) interrupts the dynamic Ras cycle. A) Top row left: Colocalization images of mCitrine-N-Ras and mCherry-H-RasC181S,C184S, which can not be palmitoylated showing palmostatin M induced mislocalization of mCitrine-N-Ras after 60 min. Similar images of mCitrine-K-Ras (top row right) and mCherry-H-RasC181S,C184S (see the Supporting Information) show no detectable redistribution at 150 min. Second row left: Intensity scatter plots of mCitrine-N-Ras and mCherry-H-RasC181S,C184S showing palmostatin M induced merging of the N-Ras and H-RasC181S,C184S pixel populations. Second row right: Intensity scatter plots show mCitrine-K-Ras maintains its localization after treatment with palmostatin M. The dotted diagonals represent theoretically identical populations. B) Top row: Colocalization images of mCitrine-H-Ras and mCherry-H-RasC181S,C184 showing minimal effect of H-Ras on the plasma membrane after 150 min, but a complete depletion of mCitrine H-Ras on the Golgi apparatus (arrows). Bottom Row: GalT-mCerulean is a Golgi marker. Scale bars represent 10 μm in all cases. C) Graph showing a comparison of the rate at which N-Ras redistributes to the unspecific localization of mCherry-HRasC181S,C184S, as quantified by Manders' correlation coefficients (*R*), upon treatment with palmostatin M (**30**; black) versus treatment with **38** (red). Trend lines are indicated.

as well as the mutant mCherry-H-RasC181S,C184S, which can not be palmitoylated, and the Golgi marker GalT mCerulean with inhibitor (1 μM) for up to 3 h. N-Ras and H-Ras are typically enriched on the Golgi and at the plasma membrane, albeit to different extents on each organelle. K-Ras is enriched on the plasma membrane through a palmitoylation-independent mechanism, while the solely prenylated H-RasC181S,C184S, which can not be palmitoylated is distributed nonspecifically in all cellular membranes.[8] We monitored the influence of the inhibitor on the redistribution of N-, H-, and K-Ras through their typical localization patterns relative to nonspecific distribution, as indicated by H-RasC181S,C184S, through confocal imaging of live cells, and quantified mislocalization through intensity correlation analysis (for details see the Supporting Information).[30] Treatment

with palmostatin M caused efficient mislocalization of N-Ras, with complete unspecific distribution reached one hour after treatment with the inhibitor. H-Ras enrichment, on the other hand, was not clearly affected at the plasma membrane on this timescale, but H-Ras was depleted from the Golgi apparatus because of the directional influence of the secretory pathway,[31] as reported before under APT1 inhibition.[7] K-Ras localization, which does not require the de/reacylation cycle[32] was completely unaffected by palmostatin M, thus indicating that palmostatin M exerts a specific effect on the acylation cycle. The results of the redistribution assays are in accordance with the phenotypic assay. Compound **38**, which showed poor phenotypic effects on transformed cells, although highly potent in the biochemical assay, was also comparably inefficient in the redistribution assay relative to palmostatin M. Complete unspecific distribution of N-Ras upon treatment with **38** at 1 μM required more than three hours, compared to less than one hour for palmostatin M (Figure 3C).

We have described the development of the APT1 inhibitor palmostatin M based on the principle of substrate similarity and its characterization in vitro and in cells. Palmostatin M perturbs the acylation cycle as well as the H- and N-Ras signaling activity at the level of depalmitoylation, thereby leading to decreased MAP-kinase signaling and partial endothelial to mesenchymal phenotypic reversion of H-Ras-transformed MDCK-F3 cells.

Palmostatin M is several times more active than palmostatin B and, as a consequence of its polar character, has a pronounced solubility yet retains cell permeability, which will allow the use of the inhibitor at substantially lower concentrations, thereby reducing the potential for unspecific effects.

Notably, for palmostatin B only APT1 has been validated as cellular target,[7] but for both palmostatin B and M the possible range of cellular targets relevant to Ras signaling has not been determined. We describe the identification of these targets by means of a reactive proteomics approach in the following manuscript.[10]

Received: April 29, 2011
Revised: August 8, 2011
Published online: September 9, 2011

Keywords: acyl protein thioesterase · inhibitors · ras protein · signal transduction

[1] J. F. Hancock, *Nat. Rev. Mol. Cell Biol.* **2003**, *4*, 373 – 385.
[2] A. Wittinghofer, H. Waldmann, *Angew. Chem.* **2000**, *112*, 4360 – 4383; *Angew. Chem. Int. Ed.* **2000**, *39*, 4192 – 4214.
[3] P. G. Dangle, B. Zaharieva, H. Jia, K. S. Pokar, *Recent Pat. Anti-Cancer Drug Discovery* **2009**, *4*, 125 – 136.
[4] M. H. Gelb, L. Brunsveld, C. A. Hrycyna, S. Michaelis, F. Tamanoi, W. C. van Voorhis, H. Waldmann, *Nat. Chem. Biol.* **2006**, *2*, 518 – 528.
[5] L. Brunsveld, J. Kuhlmann, K. Alexandrov, A. Wittinghofer, R. S. Goody, H. Waldmann, *Angew. Chem.* **2006**, *118*, 6774 – 6798; *Angew. Chem. Int. Ed.* **2006**, *45*, 6622 – 6646.
[6] O. Rocks, A. Peyker, M. Kahms, P. J. Verveer, C. Koerner, M. Lumbierres, J. Kuhlmann, H. Waldmann, A. Wittinghofer, P. I. H. Bastiaens, *Science* **2005**, *307*, 1746 – 1752.
[7] F. J. Dekker, O. Rocks, N. Vartak, S. Menninger, C. Hedberg, R. Balamurugan, S. Wetzel, S. Renner, M. Gerauer, B. Schoelermann, M. Rusch, J. W. Kramer, D. Rauh, G. W. Coates, L. Brunsveld, P. I. H. Bastiaens, H. Waldmann, *Nat. Chem. Biol.* **2010**, *6*, 449 – 456.
[8] O. Rocks, M. Gerauer, N. Vartak, S. Koch, Z.-P. Huang, M. Pechlivanis, J. Kuhlmann, L. Brunsveld, A. Chandra, B. Ellinger, H. Waldmann, P. I. H. Bastiaens, *Cell* **2010**, *141*, 458 – 471.
[9] R. Zeidman, C. S. Jackson, A. I. Magee, *Mol. Membr. Biol.* **2009**, *26*, 32 – 41, and references therein.
[10] M. Rusch, T. Zimmermann, M. Burger, F. J. Dekker, K. Görmer, G. Triola, P. Janning, T. Böttcher, S. A. Sieber, I. Vetter, C. Hedberg, H. Waldmann, *Angew. Chem.* **2011**, DOI: 10.1002/ange.201102967; *Angew. Chem. Int. Ed.* **2011**, DOI: 10.1002/anie.201102967.
[11] M. A. Koch, L.-O. Wittenberg, S. Basu, D. A. Jeyaraj, E. Gourzoulidou, K. Reinecke, A. Odermatt, H. Waldmann, *Proc. Natl. Acad. Sci. USA* **2004**, *101*, 16721 – 16726.
[12] F. J. Dekker, M. A. Koch, H. Waldmann, *Curr. Opin. Chem. Biol.* **2005**, *9*, 232 – 239.
[13] R. S. Bon, H. Waldmann, *Acc. Chem. Res.* **2010**, *43*, 1103 – 1114.
[14] A. Nören-Müller, I. Reis-Corrêa, Jr., H. Prinz, H. Rosenbaum, K. Saxena, H. J. Schwalbe, D. Vestweber, D. Cagna, S. Schunk, O. Schwarz, H. Schiewe, H. Waldmann, *Proc. Natl. Acad. Sci. USA* **2006**, *103*, 10606 – 10611.
[15] M. Kaiser, S. Wetzel, K. Kumar, H. Waldmann, *Cell. Mol. Life Sci.* **2008**, *65*, 1186 – 201.
[16] A. Wang, R. Loo, Z. Chen, E. A. Dennis, *J. Biol. Chem.* **1997**, *272*, 22030 – 22036.
[17] A. Wang, R. A. Deems, E. A. Dennis, *J. Biol. Chem.* **1997**, *272*, 12723 – 12729.
[18] H. Sunaga, H. Sugimoto, Y. Nagamachi, S. Yamashita, *Biochem. J.* **1995**, *308*, 551 – 557.
[19] T. Hirano, M. Kishi, H. Sugimoto, R. Taguchi, H. Obinata, N. Ohshima, K. Tatei, T. Izumi, *Biochim. Biophys. Acta Mol. Cell Biol. Lipids* **2009**, *1791*, 797 – 805.
[20] G. Siegel, G. Obernosterer, R. Fiore, M. Oehmen, S. Bicker, M. Christensen, S. Khudayberdiev, P. F. Leuschner, C. J. L. Busch, C. Kane, K. Hubel, F. J. Dekker, C. Hedberg, B. Rengarajan, C. Drepper, H. Waldmann, S. Kauppinen, M. E. Greenberg, A. Draguhn, M. Rehmsmeier, J. Martinez, G. M. Schratt, *Nat. Cell Biol.* **2009**, *11*, 705 – 716.
[21] J. A. Duncan, A. G. Gilman, *J. Biol. Chem.* **1998**, *273*, 15830 – 15837.
[22] Y. Shanado, M. Kometani, H. Uchiyama, S. Koizumi, N. Teno, *Biochem. Biophys. Res. Commun.* **2004**, *325*, 1487 – 1494.
[23] M. Veit, M. F. Schmidt, *Virology* **2001**, *288*, 89 – 95.
[24] Results of previous screening efforts of APT1 inhibition by β-lactones revealed the importance of a lipophilic binding motif for APT1 inhibition. For examples of compound libraries consisting of β-lactones without lipophilic substituents that did not provide any inhibition, see Z. Wang, C. Gu, T. Colby, T. Shindo, R. Balamurugan, H. Waldmann, M. Kaiser, R. A. L. van der Hoorn, *Nat. Chem. Biol.* **2008**, *4*, 557 – 562, as well as the discussion in reference [7].
[25] Y. Devedjiev, Z. Dauter, S. R. Kuznetsov, T. L. Z. Jones, Z. S. Derewenda, *Structure* **2000**, *8*, 1137 – 1146.
[26] T. Inoue, J.-F Liu, D. C. Buske, A. Abiko, *J. Org. Chem.* **2002**, *67*, 5250 – 5256.
[27] I.-M. Karaguni, P. Herter, P. Debruyne, S. Chtarbova, A. Kasprzynski, U. Herbrand, M. R. Ahmadian, K.-H. Glusenkamp, G. Winde, M. Mareel, T. Moroy, O. Muller, *Cancer Res.* **2002**, *62*, 1718 – 1723.
[28] O. Müller, E. Gourzoulidou, M. Carpintero, I.-M. Karaguni, A. Langerak, C. Herrmann, T. Moeroey, L. Klein-Hitpass, H. Waldmann, *Angew. Chem.* **2004**, *116*, 456 – 460; *Angew. Chem. Int. Ed.* **2004**, *43*, 450 – 454.

[29] J. V. Duncia, J. B. Santella III, C. A. Higley, W. J. Pitts, J. Wityak, W. E. Frietze, F. W. Rankin, J. H. Sun, R. A. Earl, A. C. Tabaka, C. A. Teleha, K. F. Blom, M. F. Favata, E. J. Manos, A. J. Daulerio, D. A. Stradley, K. Horiuchi, R. A. Copeland, P. A. Scherle, J. M. Trzaskos, R. L. Magolda, G. L. Trainor, R. R. Wexler, F. W. Hobbs, R. E. Olson, *Bioorg. Med. Chem. Lett.* **1998**, *8*, 2839 – 2844.
[30] E. Manders, F. Verbeek, J. Aten, *J. Microsc.* **1993**, *169*, 375 – 382.
[31] A. Apolloni, I. A. Prior, M. Lindsay, R. G. Parton, J. F. Hancock, *Mol. Cell. Biol.* **2000**, *20*, 2475 – 2487.
[32] K. A. Cadwallader, H. Paterson, S. G. Macdonald, J. F. Hancock, *Mol. Cell. Biol.* **1994**, *14*, 4722 – 4730.

